ELSEVIER

Journal of Electron Spectroscopy and Related Phenomena 126 (2002) 101–115

JOURNAL OF ELECTRON SPECTROSCOPY and Related Phenomena

www.elsevier.com/locate/elspec

Study of the quantum-well states in ultra-thin silver films on Si surfaces

Iwao Matsuda[a,*], Han Woong Yeom[b]

[a]*Department of Physics, School of Science, The University of Tokyo, Tokyo, Japan*
[b]*Atomic-scale Surface Science Research Center and Institute of Physics and Applied Physics, Yonsei University, Seoul, South Korea*

Abstract

The growth morphology and the electronic structures of thin metastable and epitaxial Ag films grown on Si(001)2×1 and Si(111)7×7 surfaces at low temperature were investigated by scanning tunneling microscopy and angle-resolved photoelectron spectroscopy using synchrotron radiation. The morphology of Ag films on Si(001)2×1 exhibits a strong thickness and temperature dependence, indicating an intriguing growth mechanism. The as-deposited film at ~100 K is composed of nanoclusters with flat tops in a uniform quasi-layer-by-layer film at 2–3 ML and of homogeneous clusters having a more three-dimensional (3D) character above ~5 ML. By subsequent annealing at 300–450 K, flat epitaxial Ag(111) films are formed at a nominal coverage larger than 5 ML, while a percolating network of 2D islands is formed at a lower coverage. For optimally annealed epitaxial films, discrete Ag 5*s* states are observed at binding energies of 0.3–3 eV, together with the Ag(111) surface state. The discrete electronic states are consistently interpreted by a standard description of the quantum-well states (QWSs) based on phase-shift quantization rules. The phase shift, the energy dispersion and the thickness-versus-energy relation of the QWSs of epitaxial Ag(111) films are consistently derived. The in-plane band structures of the QWSs of epitaxial Ag films grown on Si(111)7×7 and Si(001)2×1 surfaces were investigated in detail. In contrast to the expected free-electron-like behavior, the QWSs show intriguing in-plane dispersions, such as (i) a significant enhancement of the in-plane dispersion with decreasing binding energy and (ii) a splitting of a QWS into two electronic states with different dispersions at off-normal emission. Such unexpected electronic properties of a QWS are obviously related to the substrate band structure. Further, the QWS splitting is explained by the energy-dependent phase shift of the film–substrate interface occurring at the substrate band edge.

Keywords: Quantum-well states; Ultra-thin silver films; Silicon surfaces

1. Introduction

The quantum-well states (QWSs) associated with electron confinement on the nanometer scale have attracted considerable interest due to their importance in low-dimensional physics and in magnetic/electronic device applications. A well-known example is the QWSs in semiconductor/semiconductor-layered systems, which is relevant to optoelectronic devices [1,2]. Recently, many investigators have focussed on the QWSs in thin metal films grown on metal substrates, which are related to the oscillatory magnetic coupling and the giant magnetoresistance [3–9]. On the other hand, the QWSs in metal-on-semiconductor systems have received relatively little attention due partly to the difficulty of growing

*Corresponding author.

0368-2048/02/$ – see front matter
PII: S0368-2048(02)00145-7

epitaxial metal films on semiconductor substrates. However, recent scanning tunneling microscopy (STM) and low-energy electron diffraction (LEED) studies have found that continuous and atomically flat metal films can be formed even on a semiconductor substrate, for example Ag(111) films on GaAs(110) [10,11], Si(111) [12,13] and Si(001) [14,15]. Such films are prepared when Ag is deposited at a sufficiently low temperature of $<$130 K followed by mild annealing up to 300–400 K. This unique growth procedure (so-called 'two-step growth') makes it possible to study the QWS of metal-on-semiconductor systems in a systematic manner.

On the other hand, the growth mechanism of such a metastable epitaxial Ag film itself has received a great deal of interest, which features interesting critical behavior in the film thickness. The Ag films are shown to have a magic thickness of ~6 ML (1 ML$=1.39\times10^{15}$ atoms/cm^2) where the epitaxial films are formed above [10,12]. While a theoretical growth model developed recently (the so-called 'electronic growth model') invoked an important role of the QWSs within the films [16], a direct experimental study of the electronic structures of such films has been lacking. Furthermore, a much more complex growth morphology has been identified for Ag metastable films on a Si(111)7×7 surface below the critical thickness, which cannot easily be explained within the simple electronic growth model [17]. This situation obviously requires a detailed electronic structural study of metastable epitaxial films grown on a semiconductor substrate.

Angle-resolved photoelectron spectroscopy (ARPES) is a unique and direct probe of the detailed band structures of thin films. This tool has successfully revealed the presence and physical properties of the QWSs on various metal thin films [3–9,18–30]. An early ARPES study of Ag films grown on Si(111) at room temperature identified very weak QWS features [22], although later STM studies showed that such a film at room temperature is far from an ideal epitaxial film [31]. Later ARPES studies clearly observed QWSs for Ag(111) films on GaAs(110) grown by the low-temperature, two-step growth process [18,19]. However, without a morphological study of Ag films on GaAs(110), Neuhold and Horn originally interpreted the QWSs as due to Ag islands and thus no direct correlation with the film morphology could be obtained [18,19]. A very recent ARPES study also observed well-defined QWSs for Ag(111) films grown on Si(111) in a similar way, but no detailed discussion of the QWS properties was provided [13].

In this paper, we report a study of the QWSs and growth morphology of metastable Ag(111) films grown epitaxially on Si surfaces by the two-step process, that is, Ag deposition at ~100 K and subsequent annealing at 300–500 K. For a wide temperature and thickness range, the film growth mode was surveyed by LEED and reflection high-energy electron diffraction (RHEED). Using STM, the film morphology was investigated in detail at two representative Ag coverages of 2.5 and 5 ML, where significantly different types of morphology are observed. The electronic structures of the Ag films were investigated by ARPES using synchrotron radiation for thicknesses up to 30 ML. Well-defined QWSs were clearly identified at Ag film thicknesses of 5 to 30 ML. The physical properties of the QWS were studied in detail and analyzed using the well-established phase-shift quantization rule [3,21–26]. The correlation between the film structure and the QWS is discussed. We further investigated the in-plane dispersion [$E(k_{\|})$] of the QWSs of Ag(111) films on Si(111) and Si(001) with ARPES. Despite the success of the simple theoretical description of the QWS binding energies in the Ag(111)/Si(001) system, the in-plane dispersion of the QWSs exhibits a significant deviation from the expected simple free-electron-like behavior [32]. The ARPES results show a significant enhancement of the in-plane dispersion with decreasing binding energies (E_B) of the QWSs in both Ag/Si(111) and Ag/Si(001), and a splitting of a QWS into two sub-bands with different dispersions at off-normal emission in Ag/Si(001). The origins of such unexpected behavior are discussed in terms of the substrate electronic structure affecting the phase shift at the film–substrate interface.

2. Growth morphology of epitaxial Ag films on Si(001)2×1

Fig. 1a shows a STM image of the Si(001) surface with 2.5 ML Ag deposited at 65 K. We can observe a granular Ag film composed of nanoclusters with a

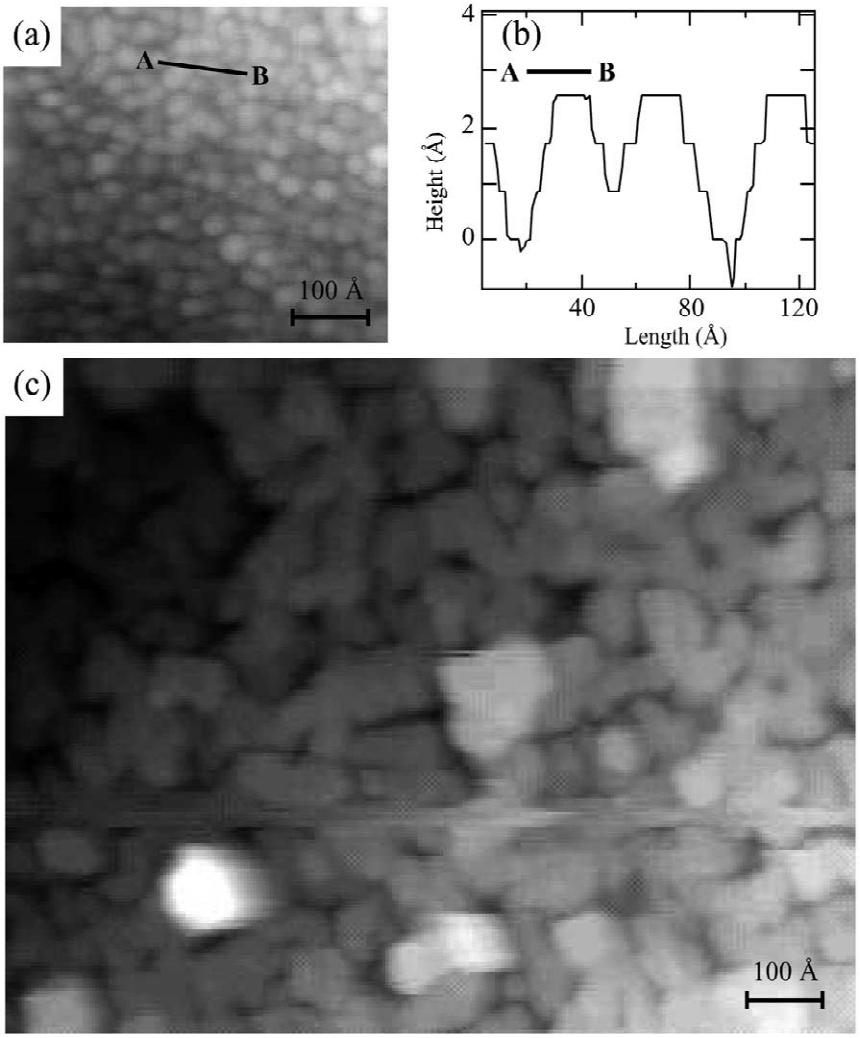

Fig. 1. (a) STM image of 2.5 ML Ag deposition on a Si(001)2×1 surface at 65 K. The image was obtained at a tip bias voltage of 5.0 V. (b) Line profile of the line A–B in (a). (c) A similar STM image for the same surface after annealing at 300 K for 1 h.

uniform size distribution of 20–30 Å, which evenly covers the whole surface. A line profile of several such clusters (the line A–B in Fig. 1a), shown in Fig. 1b, shows that the Ag nanoclusters have flat tops with sharp edges, indicating their 2-dimensional (2D) character. Within the experimental resolution, the nanoclusters likely have a uniform height difference of ~2.6 Å, which may correspond to the height of one Ag(111) layer (2.36 Å). Hence, Ag grows on Si(001)2×1 at 65 K in a quasi-layer-by-layer manner in this coverage range, although the film is composed of nanoclusters formed by the limited diffusion of Ag adsorbates. A recent LEED study observed a clear LEED intensity oscillation during Ag growth on Si(001)2×1 at 130 K [15], consistent with the above interpretation. Our own RHEED measurements also showed a clear oscillation of the (00)-spot intensity, indicating quasi-layer-by-layer growth. Such quasi-layer-by-layer growth is also reported for the growth of Ag on Si(111)7×7 at 90–150 K by STM [33] and RHEED [34]. Indeed, the STM image of Ag films of 2.5 ML grown on Si(111)7×7 at 90 K is almost identical to the present result on Si(001) [33].

For Ag deposition of 5 ML at 65 K, the nanoclusters grow in their lateral size (30–40 Å) and in height (Fig. 2a). A line profile (line C–D of Fig. 2a) shows that the shape of the nanoclusters is apparently different from those for 2.5 ML. They have sharp tops instead of flat tops and no discrete edges. This indicates that the islands start to have 3D character, which can be related to the damping of the intensity oscillations in the previous LEED study [15] and in our RHEED study upon an increase in coverage. Thus, the present STM results confirm that low-temperature Ag growth on Si(001) occurs in a quasi-layer-by-layer manner, as reported by Horn-von-Hoegen et al. [15], and in a manner similar to low-temperature Ag growth on Si(111) [34]. However, kinetic roughening of the growth front occurs to obtain a more 3D character on increasing the film thickness.

As previously reported for Ag films on GaAs(110) and Si(111), the morphology of the low-temperature-grown films is only metastable and changes drastically by mild annealing at 300–400 K. As shown in

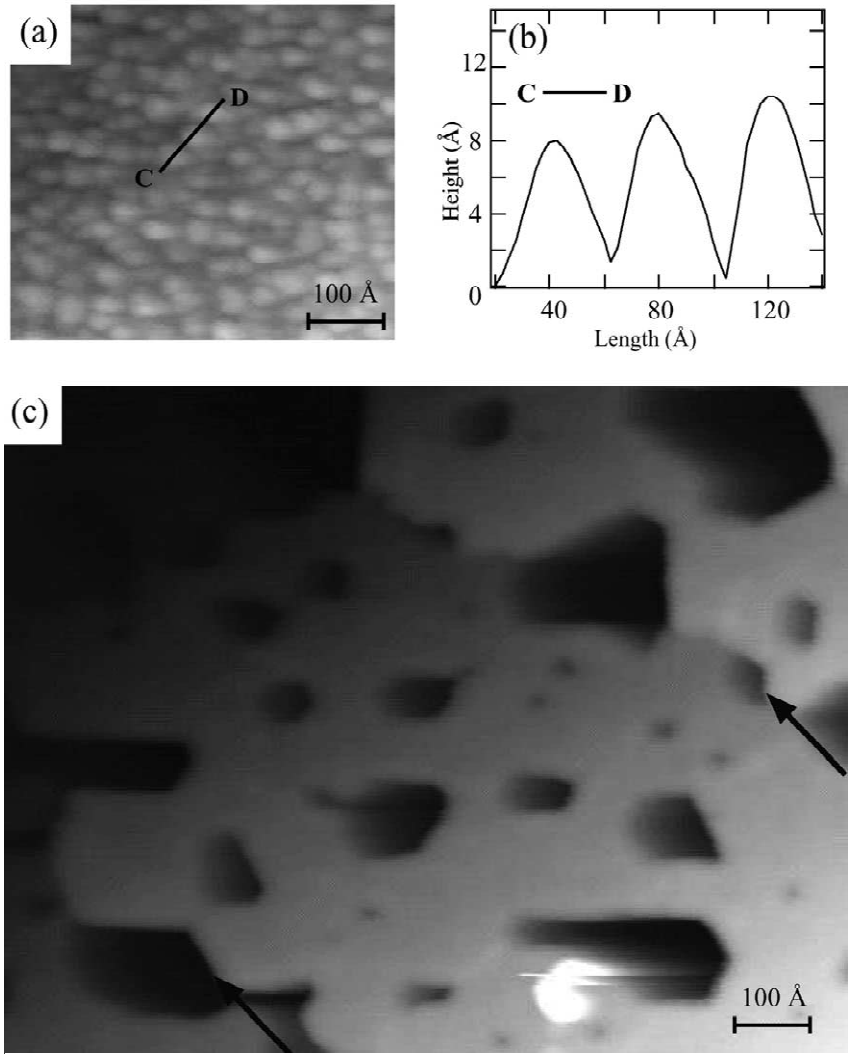

Fig. 2. (a) STM image for 5 ML Ag deposition on a Si(001)2×1 surface at 65 K obtained at a tip bias voltage of 3.0 V. (b) Line profile of the line C–D in (a). (c) A similar STM image for the same surface after annealing at 300 K for 1 h.

Fig. 1c for a 2.5 ML Ag film on Si(001) after annealing at 300 K for 1 h, a more or less irregular surface feature is observed. The film is a percolated network of 2D, atomically flat, islands of roughly ~100 Å in lateral size. The height of the 2D islands is, however, not uniform, with zero, one, two, three or even four atomic layers: roughly 60% of the islands have a height of two or three atomic layers. This STM image is similar to those for Ag films of the same coverage on Si(111)7×7 prepared in a similar procedure [12,17]. However, it can be seen that the 2D Ag islands on Si(001) have a much weaker tendency for a single height of 2 ML in contrast to those on Si(111) [12,17]. The origin of this difference is not certain at this stage, with many possible factors, such as the different surface structures of the substrates or a subtle difference in the growth conditions.

The film morphology after annealing at 300 K exhibits yet another characteristic feature, as shown in Fig. 2c. In sharp contrast to the 2.5 ML annealed film (Fig. 1c), an atomically flat Ag film is formed over the whole surface at a nominal coverage of 5 ML. The film features steps (indicated by arrows in the figure) and also 'pit holes' (dark areas in the image). The steps are identified as due to those of the Si(001) substrate by comparing the step morphology (such as the orientation and separations) with the Si(001)2×1 substrate before evaporation. That is, a flat Ag film is formed on each terrace of the Si(001) substrate without altering the substrate steps significantly. This is also confirmed by previous STM studies [14,15]. As identified by RHEED and LEED, the Ag film is a well-ordered, epitaxial Ag(111) film. The most startling feature of the film is the pit holes. It is likely that the pit holes extend down to the Si substrate as in the very similar cases of Ag epitaxial films on GaAs(110) [10,11] and Si(111) [12] grown in an identical procedure. We are now able to estimate the critical thickness of the Ag film from the surface area of the pit holes and the nominal coverage of the deposited Ag. This estimation yields a critical thickness of 6 ML, which is the same as reported previously for Ag/GaAs(110) [10] and Ag/Si(111) [12].

The above result generally favors the idea of 'electronic growth' proposed by Zhang and coworkers [16]: the Ag film is most stable at a thickness of ~5 ML, being insensitive to the strain energy imposed by the substrate due to the prevailing contribution of the quantized electrons within the film. However, as shown for Si(001) and also recently for Si(111) [12,17], Ag films on Si surfaces at the lower coverage of 2–3 ML do not share growth morphology with a critical thickness of 6 ML, in contrast to that on GaAs(110) [10,11]. On the Si(111) surface, the Ag film exhibits another critical thickness of 2 ML, i.e. a strong preference for 2 ML single-height 2D islands at a coverage of less than 3 ML [17]. Zhang and coworkers recently argued that this is also consistent with their own electronic growth model, but it was not at all clear why there should be two different critical thicknesses of 2 and 6 ML for Ag films on Si(111) [16,17]. As shown here, Ag growth on Si(001) at a coverage of less than 6 ML does not follow the expectation of the electronic growth model and does not exhibit a further critical coverage of 2 ML. While further studies are required to understand this intriguing growth mode and the dependence on the surface structure, it seems obvious that the electronic growth model oversimplifies the difference between various substrate surface structures.

3. Electronic structures of epitaxial Ag films on Si surfaces

3.1. Electronic structure along the surface normal of Ag films

An approach to the understanding of the intriguing growth morphology and the role of quantized electronic states is to study the electronic states of the films directly by ARPES. Fig. 3 shows normal-emission ARPES spectra for a Ag film with a nominal thickness of 14 ML grown on Si(001) at 120 K and for the same film but after annealing at room temperature for 1 min. Each spectrum was recorded at a photon energy ($h\nu$) of 21.0 eV. The differences of the ARPES spectra clearly indicate the drastic change of the electronic structure of the Ag film upon annealing. Without annealing, the spectral shape of the valence band near E_F is featureless (indicated as 120 K in Fig. 3). This spectral shape is similar to those of Ag deposited on Si(001)2×1 at

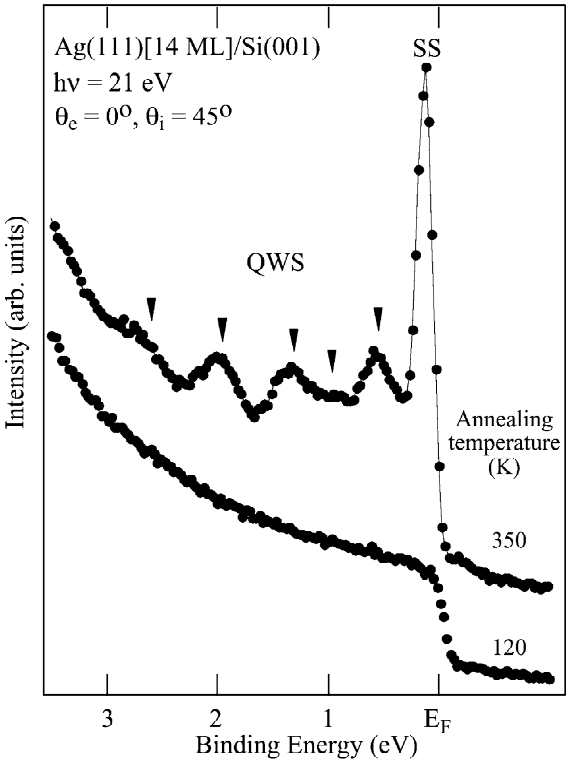

Fig. 3. A collection of normal-emission ARPES spectra for the Si(001)2×1 surface with 14 ML Ag deposited at 120 K and subsequent annealing at room temperature. The spectra were recorded at a photon energy of 21.0 eV and at a photon incident angle (θ_i) with respect to the surface normal of 45°. See text for the assignments of peaks.

room temperature with a coverage greater than 3 ML, indicating the formation of rather disordered Ag clusters [35]. The formation of such clusters for LT deposition is consistent with our STM results in Fig. 2c and with previous LEED results [15]. After annealing at 300–350 K, we observed clear (1×1) LEED and RHEED patterns of Ag(111), which is also consistent with previous STM and LEED studies, as discussed above [14,15]. The ARPES spectra after annealing show an intense structure just below E_F (denoted SS) and fine peaks at E_B of 0.3–3 eV. By comparison with ARPES studies of a clean Ag(111) surface [36] and of epitaxial Ag(111) films [21,26,27], SS can unambiguously be assigned to the surface state of the Ag(111) surface layer. As rigorously interpreted below and also by a comparison with previous ARPES studies of Ag(111) thin films [13,21,26,27], the fine peaks (the filled triangles) at an E_B of 0.3–3 eV are identified as the QWSs.

We then studied the QWSs of Ag films after annealing at 300–400 K for different Ag film thickness up to 30 ML. Fig. 4 shows a series of ARPES spectra in the energy range from E_F to the lower-binding energy tail of the Ag 4d level for

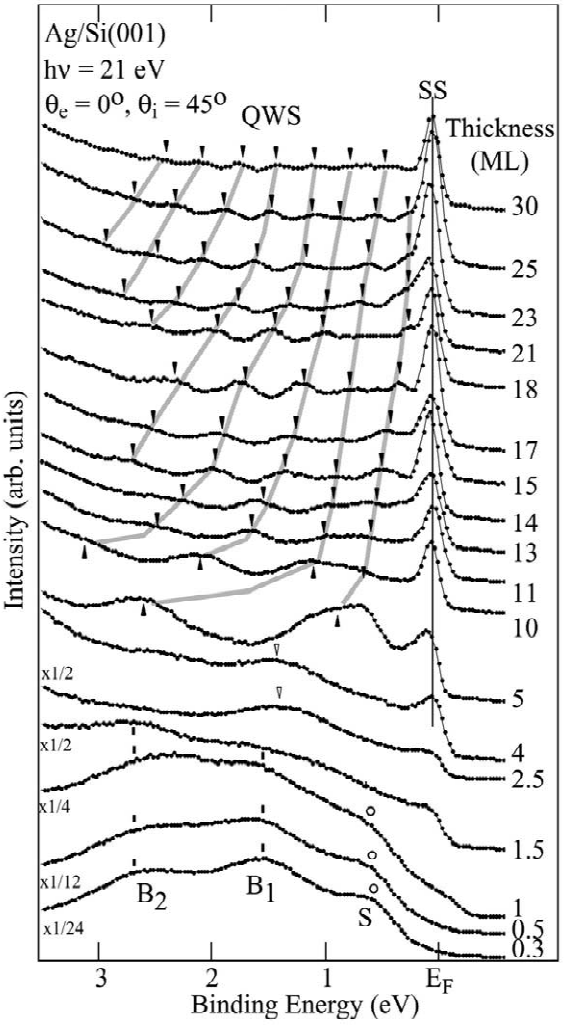

Fig. 4. Normal-emission ARPES spectra for Ag films of varying thickness on Si(001)2×1 formed by deposition at 120 K and subsequent annealing at 300–400 K. The conditions for ARPES measurements are the same as in Fig. 3. The peak positions of the quantum well states are marked with filled symbols and are traced with gray lines. See text for an explanation of the different electronic states assigned.

epitaxial Ag films of various thicknesses after annealing. At coverages of 0.3 and 0.5 ML, we find three peaks, S, B_1 and B_2, which are identified as due to the Si(001) substrate. At 1.0 ML, the density of states at E_F is observed, which is obviously due to the Ag film. This Fermi edge emission is very clear at 1.5 and 2.5 ML with a decreasing intensity of the substrate contribution. For a coverage of 4 ML, the ARPES spectra exhibit the Ag(111) surface state (SS) mentioned above. This means that the film starts to exhibit large flat surface areas with the structure of the Ag(111)1×1 surface. At coverages greater than 4 ML the SS develops further and the valence states, which are clearly different from those of the Si substrate states, are observed at binding energies of 0.3–3.0 eV (the filled symbols in Fig. 4). These states proved to be the QWS of Ag(111) films, as explained below. It is worth noting that the QWS and the SS are not clearly identified for films with a coverage of 2.5 ML. This might be related to the film morphology, as observed in the present STM study. That is, films of <3 ML exhibit only irregular 2D islands of various thickness of one to four layers, while those of ≥ 5 ML possess large, atomically flat terraces with a well-defined height.

It should be noted from our STM result (Fig. 2c) that the ARPES peaks at a nominal coverage of 5 ML correspond to the QWS of a 6 ML thick film. In Fig. 4, a systematic variation of the QWS binding energies is observed with respect to the film thickness, which is due to the change of the width of the quantum well [18–30]. In order to quantify the E_B of QWSs, several models have been used in previous studies [3,8,9,18–30,37]. We invoke the 'phase-shift quantization rule', which has been successfully applied to the interpretation of the image states and the surface states on clean metal surfaces and of the QWSs in metal thin films [8,20–27]. The quantization condition for the existence of a QWS is

$$\phi_{vac}(E_n) + 2k_{\perp}(E_n)d + \phi_{sub}(E_n) = 2\pi(n-1), \qquad (1)$$

where n is the quantum number, $k_{\perp}$ is the wave vector of the envelope function of a Bloch state perpendicular to the surface and d is the film thickness. $\phi_{vac}(E_n)$ and $\phi_{sub}(E_n)$ are the phase shifts upon reflection at the two boundaries of the film towards the vacuum and towards the substrate, respectively. The model is depicted schematically in

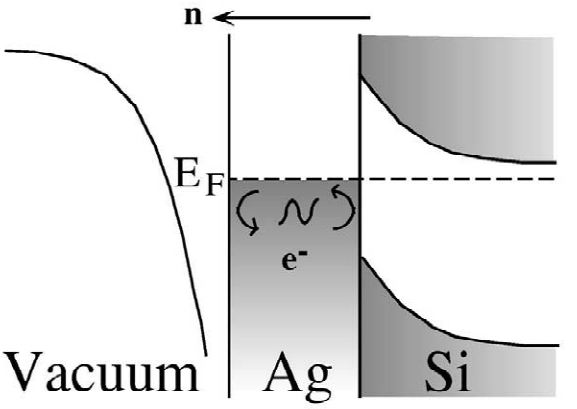

Fig. 5. Schematic drawing of electron (e^-) confinement in a Ag film between the vacuum potential and the Si substrate band gap. E_F and n indicate the Fermi level and the surface normal, respectively.

Fig. 5. In Eq. (1), $k_{\perp}(E_n)$ represents the band dispersion along the normal to the Ag(111) surface (the Γ–L direction of the 3D Brillouin zone) [23,24,26]. With a simple transformation of Eq. (1), one can derive the relationship of the thickness versus energy, the so-called 'structure plot', of the nth QWS [23,24]:

$$d_n(E_n) = [n - 1 + \phi_{vac}(E_n)/2\pi + \phi_{sub}(E_n)/2\pi]/ [1 - k(E_n)], \qquad (2)$$

where d_n is given as the number of Ag(111) atomic layers and $k(E)$ represents the bulk band dispersion in units of the size of the zone boundary wave vector at point L.

In order to solve Eq. (2), we need to know the dispersion relation of the Ag(111) *sp* band along the (111) direction, $k(E)$, and the energy dependence of the total phase shift at the two boundaries:

$$\phi_{tot}(E) = \phi_{vac}(E)/2\pi + \phi_{sub}(E)/2\pi.$$

Since $k(E)$ relates to $k_{\perp}(E)$ as $k(E) = \pi/d - k_{\perp}(E)$, one can obtain $k(E)$ from $k_{\perp}(E)$, which can be determined experimentally [26]. Briefly, if the nth quantum state for film thickness d happens to have the same binding energy as that of n' ($n' = n + 1$, for example) at thickness d', then the simultaneous solution of Eq. (1) for these two quantum states yields

$$k_{\perp} = \pi(n' - n)/(d' - d). \quad (3)$$

The $E(k_{\perp})$ data measured in this way from the present Ag(111) films are given in Fig. 6a as solid circles. The experimental dispersion is then fitted with a fitting function, which is based on the two-band nearly free electron model:

$$E(k_{\perp}) = E_0 - [ak_{\perp}^2 + U - (4a^2bk_{\perp}^2 + U^2)^{1/2}], \quad (4)$$

with $a = h^2/(8\pi^2 m^*)$ and $b = 3\pi^2/a_0^2$, $U = 4.2$ eV, the width of the band gap at the L point, and $E_0 = 0.31$, the position of the sp band edge relative to E_F [21,26]. The fit gives the electron effective mass of this band, m^*, as $(0.78)m_e$. This value is almost the same as those obtained using an identical method for the QWSs in Ag(111)/graphite(0001) [21] and in Ag(111)/Cu(111) (given as solid diamonds in Fig. 6a) [26]. The resulting dispersion curve is also in good agreement with the previous theoretical calculation for bulk Ag metal [36]. In order to fit our experimental data with Eq. (4), we used a form of the non-linear least-squares method. The error of the fitting, including the $k_{\perp}$ error, is estimated to be less than ~0.3 eV. What is left before we can solve Eq. (2) is the total phase shift, $\phi_{tot}(E)$. The typical way to find the total phase shift is to assume that ϕ_{tot} is a linear function of E [23,24] and to fit $\phi_{tot}(E)$ by putting the d_n and E_n data measured for one of the QWSs into Eq. (2) [23,24]. We chose $n = 4$ QWS since this state is observed around the center of the observed energy range and at most of the coverages. As shown in Fig. 6b, the phase shifts obtained for $n = 4$ QWS (solid squares) are fitted to $\phi_{tot}(E) = (-0.25\pi\ \text{eV}^{-1})E + 0.71\pi$.

From the empirical bulk band dispersion (Fig. 6a) and the total phase shift (Fig. 6b), the structure plots (Eq. (2)) for all QWSs are calculated as shown in Fig. 7 together with the experimental energy positions of the QWS obtained from Fig. 4. The calculated energy positions of the QWS fit the experimental data reasonably well except for $E_B < 1$ eV. The discrepancy at low E_B may originate from the rough estimation of the total phase shift. As shown in Fig. 6, the phase shift in this energy range was chosen from the linear extrapolation of the energy vs. phase shift relation determined experimentally at $E_B = 1.0$–2.5 eV. This indicates that there is possibly a

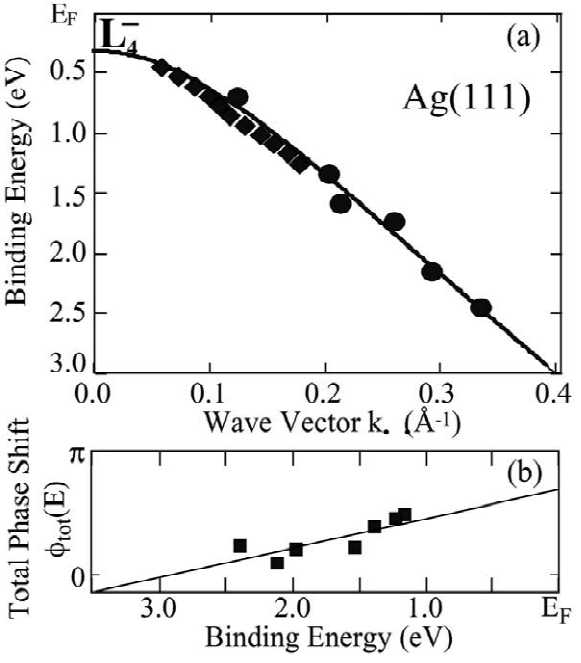

Fig. 6. (a) The sp-band dispersion for Ag bulk along the Γ–L Brillouin zone line. Data points from the present experiment on Ag(111)/Si(001) (●) and previous reports on Ag(111)/Cu(111) [26] (♦). (———) A least-squares fit of the Ag/Si(001) data points based on the two-band nearly free electron model (see text). (b) Change of the phase shift of the $n = 4$ quantum-well state of Ag(111)/Si(001) with the binding energy. Experimental data (■) and least-squares fit (———).

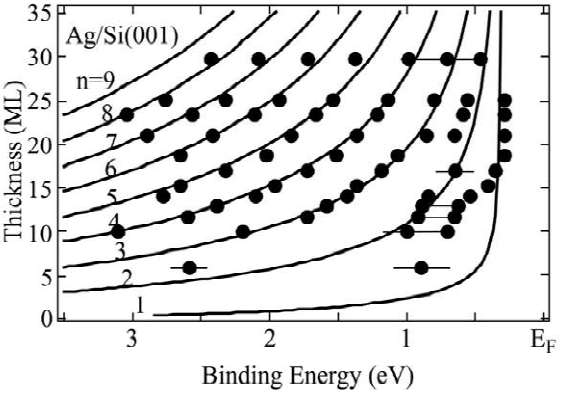

Fig. 7. Comparison between the model calculation based on the phase-quantization model (curves) and the experimental data (dots with error bars) for the binding energies of the quantum-well states for epitaxial Ag(111) films on Si(001) as a function of thickness. See text for an explanation of the model calculation.

difference in the phase shifts between our estimation and the actual shift at $E_B < 1$ eV. This would be quite reasonable since the substrate Si valence band maximum is at $E_B \sim 0.6$ eV [35,38–42], which may cause a drastic change of the phase shift at the Ag/Si interface inside and outside the substrate band gap. However, for the discrepancy of $n = 1$ QWS at a film thickness of <10 ML, we cannot exclude the possibility of a change in the Ag band structure, most likely by the strain induced by the Si(001) substrate or due to the limitation of the approximations used in obtaining the bulk dispersion. Quantitative information on the strain of such thin Ag films may also be crucial to the understanding of this issue.

Let us now return to the phase shifts at the two boundaries. The phase shift at the Ag–vacuum interface can be expressed as

$$\phi_{vac}(E) = \pi[3.4/(E_V - E)]^{1/2} - \pi, \quad (5)$$

which represents the phase shift for an image potential within the WKB approximation [43] and where E_V is the vacuum level. $\phi_{vac}(E)$ at E_F can be evaluated by introducing the work function of the Ag(111) surface (4.5 eV) into $(E_V - E)$ of Eq. (5), which yields $\phi_{vac}(E_F) = -0.13\pi$. Since $\phi_{tot}(E_F)$ was evaluated to be $\sim 0.71\pi$ (Fig. 6b), one can estimate the value of $\phi_{sub}(E_F)$ to be $\sim 0.84\pi$. Since E_F lies within the Si band gap, the electrons at E_F are Bragg-reflected at the Ag–Si interface, that is, ϕ_{sub} should ideally be π. In spite of the crude approximations used, the $\phi_{sub}(E_F)$ of Ag(111)/Si(001) obtained above is close to this expectation. In contrast, the total phase shift of the QWS of a Ag(100) film on a metal substrate was reported to be -0.4π at E_F [24]. This clearly indicates that the metal/semiconductor and the metal/metal interfaces exhibit large differences in the scattering of a Bloch-state electron near the Fermi level [44].

3.2. In-plane electronic structure of Ag films

Fig. 8 shows a gray-scale E_B–$k_\parallel$ diagram for a 16 ML thick Ag(111) film grown on Si(111)7×7. In this diagram [41,45], the spectral intensity is approximately represented by the brightness by taking the second derivative of each spectrum, which is then

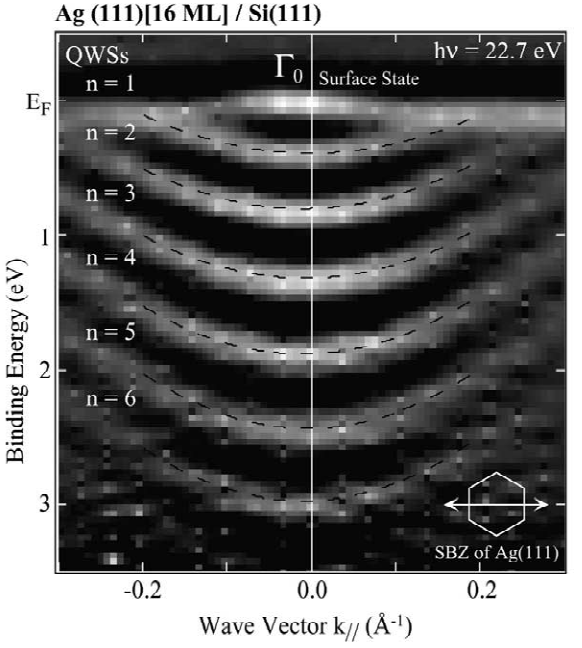

Fig. 8. Gray-scale E_B–$k_\parallel$ diagram for a 16 ML thick Ag(111) film on a Si(111) substrate along the [10$\bar{1}$] axis of the substrate recorded at $h\nu = 22.7$ eV. The surface Brillouin zone (SBZ) of the Ag(111) surface and the corresponding ARPES scan direction (the arrow) are also indicated. (- - -) Parabolic fits of the QWS dispersions as explained in the text.

mapped onto the $k_\parallel$ axis. The spectra were recorded at $h\nu = 22.7$ eV along the [10$\bar{1}$] axis of the Si substrate, which corresponds to the Γ–M line of the Ag(111)1×1 surface Brillouin zone (SBZ) (see inset of Fig. 8). In Fig. 8, one can clearly identify the parabolic dispersions of the QWSs. The dashed curves are the parabolic fits:

$$E(\boldsymbol{k}_\parallel) = h^2\boldsymbol{k}_\parallel^2/(8\pi^2 m_\parallel^*) + E_0$$

(E_0 is the binding energy at normal emission of $k_\parallel = 0$ and $m_\parallel^*$ is the in-plane effective mass), which are expected to be a good approximation for small $k_\parallel$ values [26]. Here, the fitting is performed for E_0 and $m_\parallel^*$ in the $k_\parallel$ range from -0.2 to 0.2 Å^{-1}. It is clear that the simple parabolic fits match very well with the experimental data. In addition, it was also found that the size of the in-plane dispersion decreases monotonically (i.e., $m_\parallel^*$ becomes larger) with a decrease in the QWS binding energy. That is, the

dispersion curve of the $n = 6$ QWS clearly has a larger curvature than that of $n = 1$. For example, the fitted value of $m_{\parallel}^{*}$ is $0.51m_e$ (m_e is the free electron mass) for the $n = 1$ QWS, but decreases to $0.36m_e$ for $n = 6$.

Fig. 9 summarizes the $m_{\parallel}^{*}$ values as a function of E_0, which were obtained from the above parabolic fits to the ARPES data for a 16 ML thick Ag film on Si(111). Results for 14 ML thick Ag films on Si(001) (see below) and on Cu(111) [26] are shown for comparison, together with the bulk Ag data [26] (solid line in Fig. 9). While $m_{\parallel}^{*}$ of the QWSs of Ag/Si(111) *increases* with decreasing E_0, that of Ag(111)/Cu(111) *decreases* monotonically, in clear contrast [26]. That is, the relationship between $m_{\parallel}^{*}$ and E_0 clearly exhibits an opposite tendency for the Cu(111) and Si(111) substrates. The corresponding results for the QWSs of Ag/Si(001) are described in detail below.

The above results lead to the surprising conclusion that *the in-plane band structure of a thin Ag film depends on the substrate*. In order to confirm this, we performed similar ARPES measurements for a 14 ML thick Ag(111) film grown on a Si(001)2×1 substrate. A study of Ag(111) ultrathin film growth and the QWSs on Si(001) were presented in detail above. Fig. 10 shows gray-scale E_B–$k_{\parallel}$ diagrams

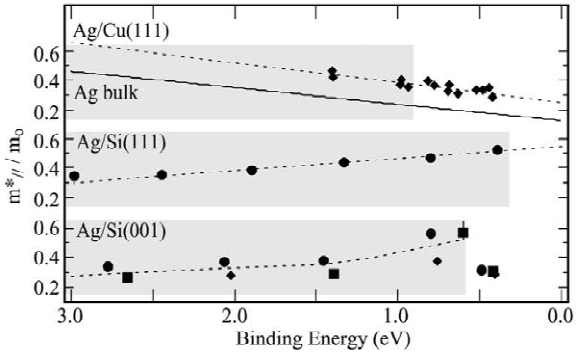

Fig. 9. Ratio of the in-plane effective mass, $m_{\parallel}^{*}$, to the free-electron mass, m_0, as a function of the QWS binding energy at $k_{\parallel} = 0$ for a Ag(111) film on Cu(111) [26], Si(111), and Si(001) substrates. (———, top panel) Estimated value for the Ag(111) bulk. (- - -) Guides for tracing the experimental data. The shaded areas correspond to the substrate valence band region. (●,■,♦, bottom panel) Data recorded at $h\nu = 22.7$, 10.3 and 9.3 eV, respectively.

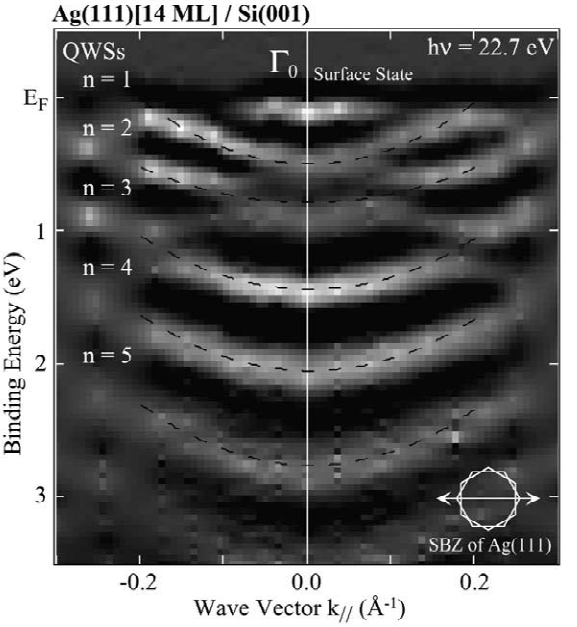

Fig. 10. Similar to Fig. 8, but for a 14 ML thick double-domain Ag(111) film on a Si(001) substrate.

recorded at a photon energy of 22.7 eV. The ARPES scans were performed along the [110] axis of the Si(001) substrate. Since the Si(001) substrate has a double-domain 2×1 surface, the Ag(111) film grows in two different orientations rotated 90° with respect to each other. Thus, the [110] axis corresponds to both the $\bar{\Gamma}$–$\bar{K}$ and $\bar{\Gamma}$–$\bar{M}$ lines of the two different Ag(111)1×1 SBZs (see inset of Fig. 10).

Since the in-plane dispersion of the Ag *sp* band is isotropic within the limited $k_{\parallel}$ range probed, these two overlapping SBZ lines do not cause any significant ambiguity for the following data analyses. Similar to Fig. 8, the Ag(111) surface state is observed just below E_F in Fig. 10. As noted in Fig. 10, while the QWS of $n = 1$ follows a normal parabolic dispersion, the $n = 2$ QWS splits into two sub-bands at $k_{\parallel} \sim \pm 0.1$ Å^{-1}; one band disperses to a lower binding energy in a roughly parabolic manner, but the other to a slightly *higher* E_B. In Fig. 10, the dashed curves are the parabolic fits to the experimental dispersions. The parabolic fits match well with the experimental data for QWSs of $n = 1$, 3, 4, and 5. For the $n = 2$ QWS, we performed a parabolic fit for the lower energy sub-band only at 0.2 Å^{-1} >

$k_{\parallel} > 0.1$ Å^{-1} and -0.2 Å$^{-1} < k_{\parallel} < -0.1$ Å^{-1} since, around Γ, the energy positions of the lower E_B sub-band are not clear and the higher E_B sub-band shows a completely different dispersion. This splitting will be discussed further below.

In order to summarize the different band dispersions of the QWSs of Ag(111) films for the different substrates, let us now return to Fig. 9. In this figure, the experimental data for Ag/Si(001) are given, together with ARPES results recorded at $h\nu = 10.3$ and 9.3 eV. In the case of Ag/Si(001), $m_{\parallel}^*$ increases monotonically as E_0 decreases to ~0.6 eV, in qualitative consistency with the case of Ag/Si(111). However, the $m_{\parallel}^*$ value becomes significantly smaller when E_0 reaches ~0.5 eV for the $n = 1$ QWS. In Fig. 9, there is a tendency for the $m_{\parallel}^*$ values obtained at $h\nu = 22.7$ eV to be slightly larger than those obtained at $h\nu = 10.3$ and 9.3 eV for Ag/Si(001). This is a systematic experimental error due to the instrumental angular resolution, which becomes poorer at higher photoelectron kinetic energies. In spite of such an error, the tendency of $m_{\parallel}^*$ is clearly shown to be invariant for the three different photon energies. The $n = 2$ QWS of Ag/Si(001) exhibits a significantly different effective mass from those of other QWSs, which is the influence of the splitting mentioned above. As is evident from Fig. 10, the in-plane dispersion of QWS is clearly and significantly different among the different substrates, Cu(111), Si(111) and Si(001).

Although the Ag *sp* valence electrons are confined and quantized one-dimensionally along the film normal in a thin Ag(111) film, the in-plane dispersion $E(\boldsymbol{k}_{\parallel})$ is expected to remain unaltered from those of bulk Ag metal. For bulk Ag(111) metal, $E(\boldsymbol{k}_{\parallel})$ is isotropic, but the size of the dispersion becomes larger with increasing E_B due to the finite hybridization with the 4*d* states at higher binding energy [32,36]. That is, $m_{\parallel}^*$ of the *sp* band increases with E_B as quantitatively estimated by Müller et al. [26] (see the solid line in Fig. 9). Such a tendency for $m_{\parallel}^*$ of the Ag bulk *sp* band was inferred to explain that of the QWSs in the Ag/Cu(111) system [26]. However, this is apparently not compatible with the present ARPES data for the Ag/Si(001) and Ag/Si(111) QWSs, which exhibit a completely opposite trend for $m_{\parallel}^*$ with respect to E_B.

A change of the in-plane dispersion might be possible due to the lateral strain of the grown film, which is naturally expected for a smooth film on a substrate with a finite lattice mismatch [46]. However, while the relaxation mechanism of the strain still remains to be elucidated, the lattice constants of Ag(111) films on Si(111) and Si(001) are reported to be very close to that of bulk Ag metal with only a few percent difference [13–15]. Within the tight-binding approximation, $m_{\parallel}^*$ is proportional to $a^{-2}\gamma(a)^{-1}$, where a is the nearest-neighbor distance and $\gamma(a)$ is the interatomic matrix element [47]. Since for *s*- and *p*-like states $\gamma(a)$ has an a^{-2} dependence [47], the strain effect on $m_{\parallel}^*$ of *sp* electrons could only be marginal. Moreover, the strain effect, if any, is naturally expected to be uniform over the whole energy region. This is obviously not the case with the present results for Ag/Si(001) and Ag/Si(111) QWSs, with a qualitatively different behavior from that of Ag bulk and Ag/Cu(111). However, we may not be able to rule out the possibility that the lattice strain changes the overall trend of the variation of $m_{\parallel}^*$ by affecting the hybridization of the Ag 4*d* and *sp* valence.

Another factor to be considered in explaining the anomalous in-plane band dispersion may be the small in-plane coherent domain size of the film. However, such a lateral size effect is unlikely, since the present Ag(111) film has a domain size larger than 200 Å as observed by STM and LEED [13–15,33], which is far beyond the quantum limit of <50 Å [48].

In a recent photoemission study of Ag overlayers on a V(100) surface, Valla et al. observed a large deviation of the Ag sp in-plane band dispersion from free-electron-like behavior [28]. They found that a QWS of a 2 ML Ag film has $m_{\parallel}^*$ as large as $3.1m_e$ in the vicinity of the Γ point and $m_{\parallel}^*$ further changes its sign when moving away from Γ. From the similarity between such an unexpected dispersion of the QWS and that of the substrate V(100) 3*d* band, Valla et al. suggested a strong hybridization between these two electronic states. Such a hybridization with the substrate electronic states may account for the unusual dispersions of the QWSs observed for Ag/Si(001) and Ag/Si(111).

In the case of Si substrates, the Si sp valence band maximum (VBM) on Γ is at $E_B \sim 0.3$ eV for Ag/Si(111) and at $E_B \sim 0.6$ eV for Ag/Si(001) [35,38–

40,49,50]. The shaded areas in Fig. 9 correspond to the substrate Si valence band region below the VBM. When a QWS is located inside this energy range, it may interact or hybridize with the substrate electronic states. It seems that the unusual behavior of the $m_{\parallel}^{*}$ of Ag/Si(001) and Ag/Si(111) occurs within such regions. We also note that the $m_{\parallel}^{*}$ values of Ag/Si(001) and Ag/Cu(111) are similar when the corresponding QWSs are located outside the substrate band region: the $n = 1$ QWS of Ag/Si(001) has $m_{\parallel}^{*} = 0.3m_{e}$ at $E_{B} = 0.5$ eV (see Fig. 9). However, the wave functions of the Ag(111) *sp* band and those of the Si(001) *sp* band are not expected to hybridize with each other due to their differenct symmetries, that is, Λ_1 for Ag(111) and Δ_5, Δ_2' for Si(001). Moreover, it is not at all clear how the hybridization affects the in-plane band dispersion of a film as thick as 14–16 ML beyond the short screening length within a metal (a few monolayers at maximum) [51,52]. A proper theoretical consideration is urgently required for the band structures of Ag films on Si substrates in order to determine the origin of the unexpected substrate-dependent in-plane dispersions.

Another unusual aspect of the in-plane dispersion of QWSs is the fact that the $n = 2$ QWS of Ag/Si(001) shows a splitting into two sub-bands with largely different dispersions (see Fig. 10). Although less obvious, similar splittings can be observed for other quantum numbers such as $n = 3$ in Fig. 10. In considering the origin of these split bands, we can exclude the possibility of observing photoemission from the substrate surface. This is because (i) the STM and electron diffraction results [14,15] clearly show that the Ag(111) film covers the terraces of the substrate surface uniformly, and (ii) the electron mean free path for the corresponding photoelectrons is ~10 Å at most [53], which amounts to only about one-third of the thickness of the present Ag(111) films. Thus, the unusual Ag QWS dispersion has to be attributed to the electronic states of the Ag film itself. One may suspect that the above splitting may be due to the mixed contributions from the parts of the Ag films of different thicknesses. This explanation is not plausible either, since: (i) the Ag films are shown to be uniform with only ±1 or 2 ML height variation; (ii) the expected energy splitting from such a height variation is much smaller than observed [4,6]; and (iii) the expected dispersion of QWSs from a slightly different film thickness should still follow a parabolic dispersion in contrast to the present observation. Similar splittings are also observed for Ag(111) films on Si(001) with different thicknesses.

We now discuss the peculiar splitting of the QWSs observed for Ag/Si(001) in terms of the quantization condition of a QWS within the phase quantization rule [3,8,23–26,30]. Eq. (1) gives the phase shift at the film–vacuum or the film–substrate interface. For a QWS of a certain thickness, the dispersion normal to the surface, $k_{\perp}(E_n)$, depends on the phase shifts. This is very similar to what is known for the dispersion of the so-called image-potential states of clean metal surfaces [54]. Thus, if $\phi_{sub}(E_n)$ or $\phi_{vac}(E_n)$ changes with $k_{\parallel}$, then the binding energy of a QWS would depend on $k_{\parallel}$ in addition to its own parabolic dispersion given by the bulk *sp* band structure. In particular, near the edge of the substrate bands, $\phi_{sub}(E_n)$ can vary drastically between the outside and the inside of the substrate band. This discontinuity of the phase shift is expected to distort the $E(\boldsymbol{k}_{\parallel})$ dispersion curve away from free-electron-like behavior, bringing about a splitting or a discontinuity of the QWS dispersion at the bulk valence band edge. Consistent with this argument, it can be seen from Fig. 10 that the positions of the QWS energy splitting coincide reasonably well with the upper edge of the Si(001) valence bands [35,38–40].

More quantitatively, the splitting is observed at $k_{\parallel} \sim \pm 0.1$ Å^{-1} and at $E_{B} \sim 0.8$ eV for the $n = 2$ QWS (Fig. 10). Based on the one-dimensional potential well model [55], $\phi_{sub}(E_n)$ inside the Si valence band is treated as a constant, which is estimated experimentally to be $\phi_{sub} \sim 0.7\pi$ for the $n = 2$ QWS (Fig. 6b). Within the band gap, $\phi_{sub}(E_n)$ is presumably π, as in the case of a perfect Bragg reflection. Then, the difference in phase shift between the outside and inside of the substrate band corresponds to 0.3π and the phase quantization rule gives

$$\Delta\phi_{vac}(E_n) + 2\Delta k_{\perp}(E_n)d = 0.3\pi,$$

where $\Delta\phi_{vac}(E_n)$ and $\Delta k_{\perp}(E_n)$ are the differences of $\phi_{vac}(E_n)$ and $k_{\perp}(E_n)$, respectively, between the out-

side and the inside of the substrate band at $E_B \sim 0.8$ eV. Since $\phi_{vac}(E_n)$ is not expected to depend on the Si band structure, the $\Delta\phi_{vac}(E_n)$ term should be negligible compared to the $2\Delta k_\perp(E_n)d$ term. Although $\phi_{vac}(E_n)$ is, in principle, energy dependent, it is, however, estimated to be negligibly small compared to the change in $\phi_{sub}(E_n)$ within the WKB approximation [43]. $\Delta k_\perp(E_n)$ is then reduced to -0.015 Å^{-1} and the corresponding E_B discontinuity for the $n=2$ QWS is estimated to be -0.10 ± 0.04 eV from the $k_\perp(E_n)$ relation obtained previously (Fig. 6a). This value agrees reasonably well with the observed energy splitting of -0.13 ± 0.03 eV for the $n=2$ QWS (Fig. 10). Similar estimations were also made for the $n=3$ and 4 QWSs in agreement with the observed energy splittings; for example, 0.13–0.18 eV for $n=3$. These estimations corroborate the idea of a phase shift discontinuity at the substrate band edge in explaining QWS splitting at off-normal emission. However, the simple model presented here is not sufficiently complete to describe the detailed dispersion of the split QWS as observed for the higher energy branch of the $n=2$ QWS.

If we assume a similar relationship of the energy and the phase shift for Ag/Si(001) and Ag/Si(111), the change in E_B of the QWS at the Si bulk band edge around $E_B \sim 0.5$ eV [the $n=1$ QWS of Ag/Si(111)] is only -0.03 ± 0.03 eV. Such a small value is due to flattening of the Ag *sp* band near the band top. Such a small splitting and the broad QWS peak width may explain why we do not observe any obvious QWS spitting for Ag/Si(111), as shown in Fig. 8.

4. Conclusions

The low-temperature growth and electronic structure of thin metastable Ag films on Si(001)2×1 and Si(111)7×7 surfaces were investigated by STM and ARPES using synchrotron radiation. The as-deposited film at ~100 K is composed of 2D nanoclusters in a uniform quasi-layer-by-layer film at 2–3 ML, which changes into larger clusters with more 3D character at ~5 ML. These clusters possess a uniform size distribution of 20–30 and 30–40 Å at 2.5 and 5 ML, respectively. This morphology is altered drastically by subsequent annealing at 300–450 K into two characteristically different structures. A percolating network of 2D islands of ~100 Å size is formed at 2.5 ML with rather disordered heights. In sharp contrast, atomically flat epitaxial Ag(111) films are formed at a nominal coverage greater than 5 ML. The growth morphology seems to be consistent with the recently introduced electronic growth model of a critical thickness of 6 ML at high coverages. However, discrepancy with this growth model is obvious at a lower coverage.

The ARPES spectra also exhibit a drastic change upon annealing. With optimal annealing at 300–450 K, epitaxial Ag(111) films of 6–30 ML are formed with a well-defined QWS of the Ag 5*s* band at binding energies of 0.3–3 eV together with the Ag(111) surface state. No such well-defined QWS is observed for films with a coverage of less than ~5 ML, which is most likely related to the different morphology at low coverage as observed by STM. The QWSs are consistently analyzed within the standard phase-shift quantization model. The phase shift of the QWS at E_F in the Ag/Si interface is estimated to be close to π, indicating a far more perfect reflection of Bloch waves than a Ag/metal interface. The phase shift, the energy dispersion and the thickness-versus-energy relation (structure plots) of the QWS of epitaxial Ag(111) films are consistently derived.

The in-plane dispersions of QWSs have been studied extensively for epitaxial Ag(111) films grown on Si(001) and Si(111) by angle-resolved photoemission. The QWSs show unexpected dispersions that deviate significantly from those expected from the bulk Ag *sp* band. That is, the QWS exhibits a splitting into two branches with largely different dispersions at off-normal emission, and the in-plane effective mass, $m_\parallel^*$, shows a significant enhancement with decreasing QWS binding energy. This behavior is found to be closely related to the substrate band structure and the splitting can be discussed in terms of the discontinuity of the reflection phase shift of the Ag/Si interface occurring at the valence band edge of the substrate. Further investigations, such as theoretical calculations, are required for a better and quantitative understanding of the peculiar QWS properties observed.

Acknowledgements

This work was performed with Mr. T. Tanikawa, Mr. K. Tono, Prof. S. Hasegawa, Prof. T. Nagao, and Prof. T. Ohta. The authors are also grateful to Mr. K. Horikoshi and S. Ouchi for their help during the STM experiments. I.M. gratefully acknowledges financial support from the Photon Factory via Prof. A. Yagishita and from the Japan Society for the Promotion of Science. H.W.Y. was supported by ASSRC, funded by KOSEF, the Brain Korea 21 program, and the Tera-level Nanodevices project (21st century Frontier Programs).

References

[1] R.M. Kolbas, N. Holonyak, Am. J. Phys. 52 (1984) 431.
[2] R.C. Jaklevic, J. Lambe, Phys. Rev. B 12 (1975) 4146.
[3] T.-C. Chiang, Surf. Sci. Rep. 39 (2000) 181.
[4] J.J. Paggel, T. Miller, T.-C. Chiang, Phys. Rev. B 61 (2000) 1804.
[5] D.-A. Luh, J.J. Paggel, T. Miller, T.-C. Chiang, Phys. Rev. Lett. 84 (2000) 3410.
[6] J.J. Paggel, T. Miller, T.-C. Chiang, Science 283 (1999) 1709.
[7] F.J. Himpsel, Science 283 (1999) 1655.
[8] R.K. Kawakami, E. Rotenberg, E.J. Escorcia-Aparicio, H.J. Choi, T.R. Cummins, J.G. Tobin, N.V. Smith, Z.Q. Qiu, Phys. Rev. Lett. 80 (1998) 1754.
[9] F.J. Himpsel, Surf. Rev. Lett. 2 (1995) 81.
[10] A.R. Smith, K.-J. Chao, Q. Niu, C.-K. Shih, Science 273 (1996) 226.
[11] G. Neuhold, L. Bartels, J.J. Paggel, K. Horn, Surf. Sci. 376 (1997) 1.
[12] L. Huang, S.J. Chey, J.H. Weaver, Surf. Sci. 416 (1998) L1101.
[13] G. Neuhold, K. Horn, Phys. Rev. Lett. 78 (1997) 1327.
[14] M.H.-v. Hoegen, T. Schmidt, M. Henzler, G. Meyer, D. Winau, K.H. Rieder, Phys. Rev. B 52 (1995) 10764.
[15] M.H.-v. Hoegen, T. Schmidt, M. Henzler, G. Meyer, D. Winau, K.H. Rieder, Surf. Sci. 331–333 (1995) 575.
[16] Z. Zhang, Q. Niu, C.-K. Shih, Phys. Rev. Lett. 80 (1998) 5381.
[17] L. Gavioli, K.R. Kimberlin, M.C. Tringides, J.F. Wendelken, Z. Zhang, Phys. Rev. Lett. 82 (1999) 129.
[18] D.A. Evans, M. Alonso, R. Cimino, K. Horn, Phys. Rev. Lett. 70 (1993) 3483.
[19] D.A. Evans, K. Horn, Surf. Sci. 307–309 (1994) 321.
[20] M. Jalochowski, H. Knoppe, G. Lilienkamp, E. Bauer, Phys. Rev. B 46 (1992) 4693.
[21] F. Patthey, W.-D. Schneider, Phys. Rev. B 50 (1994) 17560.
[22] A.L. Wachs, A.P. Shapiro, T.C. Hsieh, T.-C. Chiang, Phys. Rev. B 33 (1986) 1460.
[23] J.E. Ortega, F.J. Himpsel, G.J. Mankey, R.F. Willis, Surf. Rev. Lett. 4 (1997) 361.
[24] J.E. Ortega, F.J. Himpsel, G.J. Mankey, R.F. Willis, Phys. Rev. B 47 (1993) 1540.
[25] N.V. Smith, Phys. Rev. B 49 (1994) 332.
[26] M.A. Müller, T. Miller, T.-C. Chiang, Phys. Rev. B 41 (1990) 5214.
[27] T. Miller, A. Samsavar, T.-C. Chiang, Phys. Rev. B 50 (1994) 17686.
[28] T. Valla, P. Pervan, M. Milun, A.B. Hayden, D.P. Woddruff, Phys. Rev. B 54 (1996) 11786.
[29] W.E. McMahon, T. Miller, T.-C. Chiang, Phys. Rev. B 54 (1996) 10800.
[30] S.Å. Lindgren, L. Wallden, Phys. Rev. Lett. 59 (1987) 3003.
[31] S. Tosch, H. Neddermeyer, Phys. Rev. Lett. 61 (1988) 349; H. Neddermeyer, Crit. Rev. Solid State Mater. Sci. 16 (1990) 309.
[32] H. Erschbaumer, A.J. Freeman, C.L. Fu, R. Podloucky, Surf. Sci. 243 (1991) 317.
[33] G. Meyer, K.H. Rieder, Appl. Phys. Lett. 64 (1994) 3560; G. Meyer, K.H. Rieder, Surf. Sci. 331–333 (1995) 600.
[34] Z.H. Zhang, S. Hasegawa, S. Ino, Phys. Rev. B 55 (1997) 9983.
[35] I. Matsuda, H.W. Yeom, K. Tono, T. Ohta, Surf. Sci. 438 (1999) 231.
[36] H. Wern, R. Courths, G. Leschik, S. Hüfner, Z. Phys. B 60 (1985) 293.
[37] A. Beckmann, M. Klaua, K. Meinel, Phys. Rev. B 48 (1993) 1844.
[38] H.W. Yeom, I. Matsuda, K. Tono, T. Ohta, Phys. Rev. B 57 (1998) 3949.
[39] I. Matsuda, H.W. Yeom, K. Tono, T. Ohta, Phys. Rev. B 59 (1999) 15784.
[40] L.S.O. Johansson, R.I.G. Uhrberg, P. Martensson, G.V. Hansson, Phys. Rev. B 42 (1990) 1305.
[41] H.W. Yeom, T. Abukawa, Y. Takakuwa, M. Nakamura, M. Kimura, A. Kakizaki, S. Kono, Surf. Sci. Lett. 321 (1994) L177.
[42] H.W. Yeom, T. Abukawa, Y. Takakuwa, Y. Mori, T. Shimatani, A. Kakizaki, S. Kono, Phys. Rev. B 53 (1996) 1948.
[43] E.G. McRae, M.L. Kane, Surf. Sci. 108 (1981) 435.
[44] J. Holzl, F.K. Schulte, H. Wagner, Work function of metals, in: Solid Surface Physics, Springer Tracts in Modern Physics, Vol. 85, Springer, Berlin, 1979.
[45] T. Abukawa, M. Sasaki, T. Hisamatsu, T. Goto, T. Kinoshita, A. Kakizaki, S. Kono, Surf. Sci. 325 (1995) 33.
[46] E. Bauer, J. van der Merwe, Phys. Rev. B 33 (1986) 3657.
[47] W.A. Harrison, Electronic Structure and the Properties of Solids, Dover, 1989;
S. Froyen, W.A. Harrison, Phys. Rev. B 20 (1979) 2420.
[48] R. Fischer, Th. Fauster, W. Steinmann, Phys. Rev. B 48 (1993) 15496.
[49] S. Hasegawa, X. Tong, S. Takeda, N. Sato, T. Nagao, Prog. Surf. Sci. 60 (1999) 89.
[50] G.L. Ley, V.Yu. Aristov, L. Seehofer, T. Buslaps, R.L. Johnson, M. Gothelid, M. Hammar, U.O. Karlsson, S.A.

Flodstroem, R. Feidenhans'l, M. Nielsen, E. Findeisein, R.I.G. Uhrberg, Surf. Sci. 307–309 (1994) 280.
[51] A. Zangwill, Physics at Surfaces, Cambridge University Press, 1988.
[52] H. Lüth, Surface and Interfaces of Solid Materials, Springer, Berlin, 1993, 1995.
[53] S. Hüfner, Photoelectron Spectroscopy, Springer Series in Solid-State Sciences, Vol. 82, Springer, Berlin, 1995.
[54] H. Eckhardt, L. Fritsche, J. Noffke, J. Phys. F 14 (1984) 97.
[55] P. Harrison, Quantum Wells, Wires and Dots, Wiley, New York, 2000.